Journal of Advanced Research (2015) 6, 711–720

Cairo University

Journal of Advanced Research

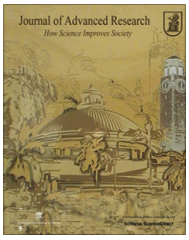

ORIGINAL ARTICLE

An eco-friendly method of synthesizing gold nanoparticles using an otherwise worthless weed pistia (*Pistia stratiotes* L.)

J. Anuradha, Tasneem Abbasi [1], S.A. Abbasi *

Centre for Pollution Control and Environmental Engineering, Pondicherry University, Puducherry 605 014, India

ARTICLE INFO

Article history:
Received 4 December 2013
Received in revised form 7 March 2014
Accepted 28 March 2014
Available online 13 April 2014

Keywords:
Biomimetics
Pistia stratiotes
Gold nanoparticles
Anisotropy

ABSTRACT

A biomimetic method of gold nanoparticles synthesis utilizing the highly invasive aquatic weed pistia (*Pistia stratiotes*) is presented. In an attempt to utilize the entire plant, the efficacy of the extracts of all its parts – aerial and submerged – was explored with different proportions of gold (III) solution in generating gold nanoparticles (GNPs). The progress of the synthesis, which occurred at ambient temperature and pressure and commenced soon after mixing the pistia extracts and gold (III) solutions, was tracked using UV–visible spectrophotometry. The electron micrographs of the synthesized GNPs revealed that, depending on the metal-extract concentrations used in the synthesis, GNPs of either monodispersed spherical shape were formed or there was anisotropy resulting in a mixture of triangular, hexagonal, pentagonal, and truncated triangular shaped GNPs. This phenomenon was witnessed with the extracts of aerial parts as well as submerged parts of pistia. The presence of gold atoms in the nanoparticles was confirmed from the EDAX and X-ray diffraction studies. The FT-IR spectral study indicated that the primary and secondary amines associated with the polypeptide biomolecules could have been responsible for the reduction of the gold (III) ions to GNPs and their subsequent stabilization.

Introduction

Metal nanoparticles have been the focus of a large body of scientific research due to the fact that their catalytic activity and their antimicrobial, electronic, optical, magnetic and medical properties are often significantly different from that of the bulk materials. Given that nanoparticles of different metals have several unique properties, and that these properties further depend on the morphology and size of the nanoparticles, it has become essential to develop methods with which nanoparticles of desired shape and sizes can be generated. The traditional methods of doing it revolve round chemical or physical techniques. Of these, the former often involve hazardous reagents and/or process conditions and lead to emission of pollutants. The latter are highly energy-intensive and expensive. In contrast, biological methods which employ biomolecules contained in microorganisms, algae, or vascular plants to generate nanoparticles in a way similar to that which occurs in nature – i.e. by biomimetics – are much cleaner and

* Corresponding author. Tel.: +91 413 2654398.
E-mail address: prof.s.a.abbasi@gmail.com (S.A. Abbasi).
[1] Concurrently Visiting Associate Professor, Department of Fire Protection Engineering, Worcester Polytechnic Institute, Worcester, MA 01609, USA.

Peer review under responsibility of Cairo University.

2090-1232 © 2014 Production and hosting by Elsevier B.V. on behalf of Cairo University.
http://dx.doi.org/10.1016/j.jare.2014.03.006

'greener'. This aspect has bestowed great relevance to the field of biomimetic nanoparticles synthesis [1–6].

The use of botanical species (henceforth referred to as 'plants') in the synthesis of nanoparticles has several advantages compared to methods relying on microorganisms as the agent brining about the synthesis. The latter require elaborate effort for maintaining microbial cultures and carry the hazard of leaks, which can endanger the environment and the human health. Microbial nanoparticle synthesis methods do not, also, lend themselves easily to large-scale processing. Moreover, the time required for microorganism-mediated nanoparticle synthesis can be very long, going up to 120 h [7,8]. The difficulties associated with maintaining the microbial cultures [9,10] further depreciates the value of this synthesis route in favor of plant-based procedures.

So far different authors have used about 130 species of plants to generate gold nanoparticles (GNPs). These species encompass fruits, flowers, vegetables, grains, cereals, spices, other foodstuff, medicinal plants, and beauty aids. For example, geranium, neem, gooseberry, aloe vera, coriander, guava, clove buds, mint, cinnamon, curry leave, aloe, horse gram, myrobalan, white gourd and citrus fruit that already have well-established uses, and entail substantial costs of production, have been explored [2,4,6,11,12]. Also, in the past, most authors have used only one or the other part of the plants (leaf/bark/seed/flower/fruit) for GNP synthesis. In contrast, the present study is based on the use of whole plant of a highly pernicious weed, pistia (*Pistia stratiotes*). It is a free-floating pleustonic macrophyte belonging to the Araceae family. It is one among the world's worst weeds and is now widespread in the lakes and ponds of the warmer parts of the world, seriously harming water quality and endangering biodiversity [13,14]. Given this context, the method presented here opens an avenue for the gainful utilization of pistia. The ability of the method to utilize the whole plant is significant because on one hand it enhances the utility value of each plant and on the other hand it makes the utilization of the invasive so potentially gainful that it may become remunerative to control the invasive through its harvesting and use. Hence, the present study can have far-reaching beneficial portent for the protection of large tracts of aquatic ecosystems currently plagued with pistia.

Table 1 Wavelengths of absorption peaks (λ_{max}, nm) and corresponding absorbance of gold nanoparticle suspensions synthesized using extracts of pistia.

Plant part used for preparing the extract	Metal: extract concentration ratio	Reaction duration (h)											
		2		4		6		24		48			
		λ_{max}	Absorbance	λ_{max}	Absorbance	λ_{max}	Absorbance	λ_{max}	Absorbance	λ_{max}	Absorbance		
Aerial	1:5	670	0.171	707	0.279	705	0.353	558	0.411	558	0.424		
	1:6	644	0.247	792	0.344	600	0.455	552	0.522	543	0.455		
						1018	0.508	1070	0.608	1023	0.503		
	1:7	–	–	549	0.782	542	1.035	554	0.821	550	0.784		
	1:10	–	–	539	0.739	543	0.789	549	0.754	550	0.727		
	1:15	–	–	549	0.362	541	0.539	548	0.487	549	0.453		
	1:30	531	0.189	535	0.216	535	0.225	539	0.238	540	0.208		
Submerged	1:5	–	–	–	–	–	–	567	0.630	562	0.541		
	1:6	–	–	–	–	–	–	568	0.609	562	0.514		
	1:7	561	1.068	546	1.288	545	1.292	544	1.434	543	1.365		
		912	1.189	985	1.752	960	1.795	909	2.021	877	1.893		
	1:10	551	1.535	550	1.683	548	1.684	543	1.754	543	1.702		
				686	1.438	675	1.451	655	1.518	645	1.478		
	1:15	531	1.720	531	1.799	531	1.791	531	1.805	531	1.807		
	1:30	531	1.135	530	1.159	529	1.153	528	1.202	530	1.224		

Experimental

All chemicals were of analytical grades unless specified otherwise. Deionized, double-distilled water was used throughout.

Preparation of aqueous extracts of the aerial and submerged parts of pistia

Pistia was collected from the ponds situated near the campus of Pondicherry University, Puducherry. The fresh, mature, and disease-free plant portions were washed thoroughly with water and then dipped in saline water to sterilize their surface, followed by washing liberally before blotting them dry. A known quantity of plant samples was dried at 105 °C to a constant weight [15]. On the basis of dry weight thus obtained, extracts for nanoparticle synthesis were made by boiling 1.0 g dry weight equivalent plant material with 100 ml of water for 5 min. The contents were filtered through a Whatmann number. A Whatman No. 42 filter paper and the filtrate were

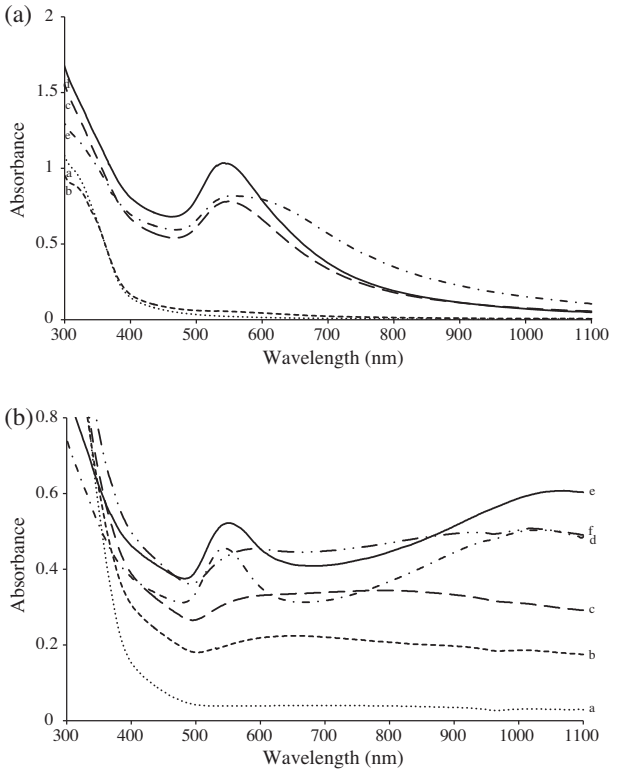

Fig. 1 Typical UV–visible spectra of gold nanoparticles formed using the aqueous extract of the aerial parts of pistia: (a) of monodispersed spherical GNPs; (b) of polydispersed anisotropic GNPs.

stored under refrigeration at 4 °C [4,16]. Reconnoitery experiments indicated that the extracts retained their integrity for up to 3 days, as evidenced by the extent of intensity of nanoparticles generated by them. Hence, in all the experiments, the extracts were used within 3 days of preparation.

Au (III) solution

A 10^{-3} M solution of Au (III) was prepared with $HAuCl_4$. It was stored in amber bottles covered with black sheets.

Nanoparticle synthesis

The plant extracts were mixed with Au (III) solution at ambient temperature. The GNPs began forming almost immediately as indicated by the appearance of pinkish red or purple color which grew in intensity with time. The spectra of the reaction mixtures were continuously recorded using UV–visible spectrophotometer and indicated that the hue of the color and its intensity depended on the stoichiometric ratio in which the plant extract and the metal ion had been mixed. Metal: extract combinations varying in concentration from 1:1 to 1:40 were explored. Typical results, of six of the combinations, are given in Table 1.

Characterization of the GNPs

UV–visible spectroscopy

The nanoparticle formation was monitored by recording the UV–vis spectra in the wavelength range 190–1100 nm employing Labindia (model UV 3000^+) and ELICO (model SL 164) double beam UV–visible spectrophotometers operated at 1 nm resolution (Figs. 1 and 2). Typical results of the λ_{max} and absorbance are presented in Table 1.

SEM/TEM studies

SEM (scanning electron microscopy) and TEM (transmission electron microscopy) studies were carried out to determine the size and morphology of the synthesized GNPs. The reactant–GNP mixtures were centrifuged at 12,000 rpm for 20 min using Remi C 24 centrifuge. The resulting pellets were washed thrice with water to remove the unreacted constituents and were re-dispersed in water. SAED (selected area electron diffraction) studies were done in conjunction with TEM to assess the crystalline nature of the GNPs.

The samples for SEM studies were prepared by placing a drop of suspension on a carbon-coated SEM grid. For high resolution SEM studies, the samples were prepared by placing dried pellets on a carbon coated aluminum stub. For TEM studies, the GNPs were pelletized by centrifuging and through sonication. The micrographs were recorded by depositing a drop of the well-dispersed samples on carbon coated 300 mesh placed on copper TEM grids.

Energy dispersive X-ray (EDAX) studies

The elemental composition of the GNPs was assayed using the EDAX equipment attached with the SEM/HRSEM microscopes. The EDAX spectrum was recorded after documenting

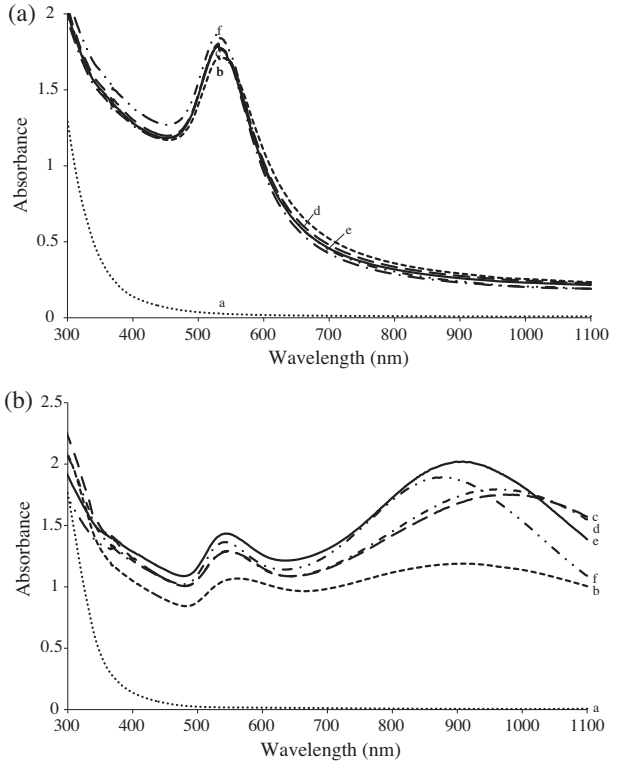

Fig. 2 Typical UV–visible spectra of gold nanoparticles formed using the aqueous extract of the submerged parts of pistia: (a) of monodispersed spherical GNPs; (b) of polydispersed anisotropic GNPs.

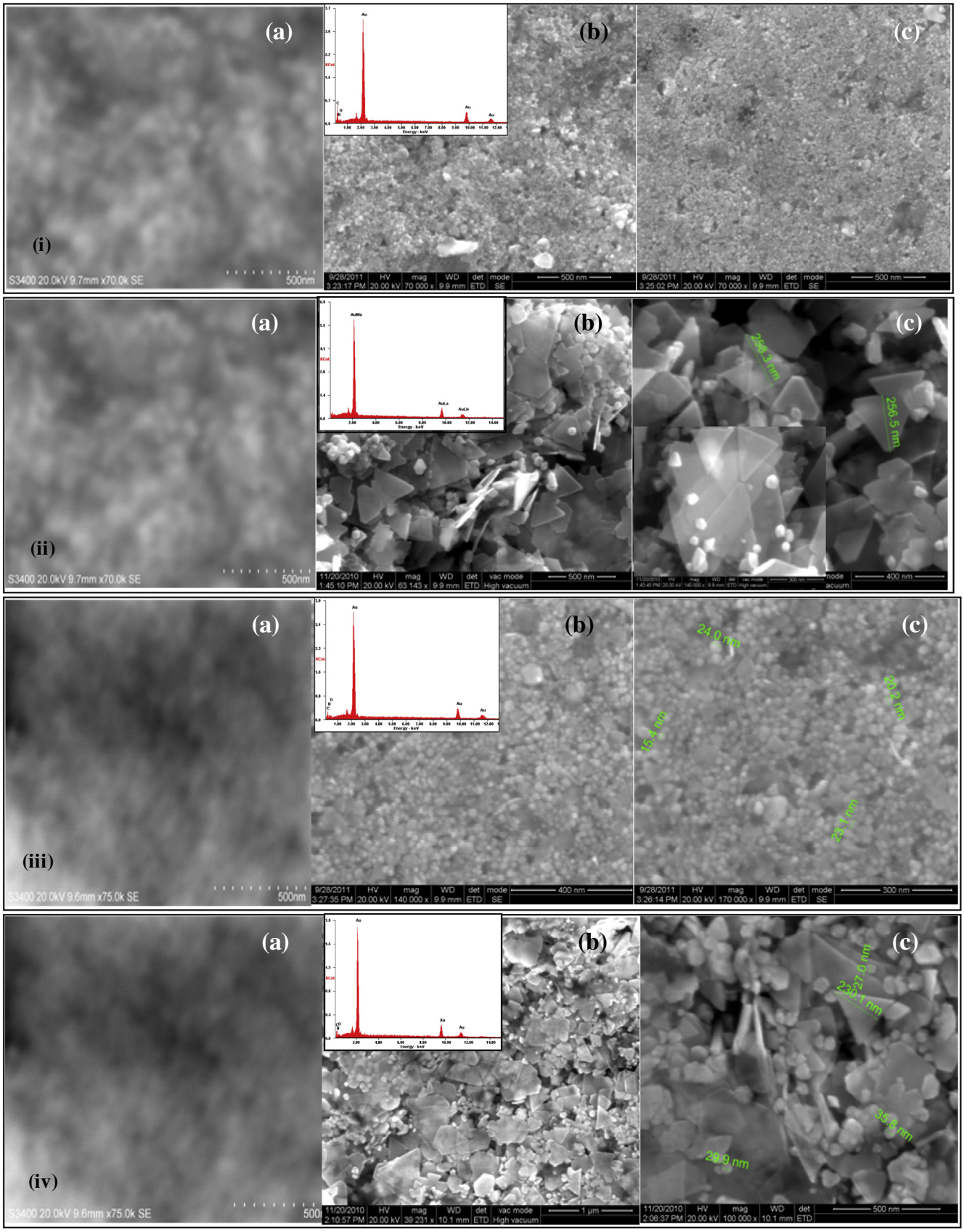

Fig. 3 A composite visual of (a) scanning electron micrograph; (b and c) high resolution scanning electron micrographs (inset is the EDX spectrum) of gold nanoparticles formed with the extracts of the aerial parts (i and ii), and submerged parts (iii and iv) of pistia.

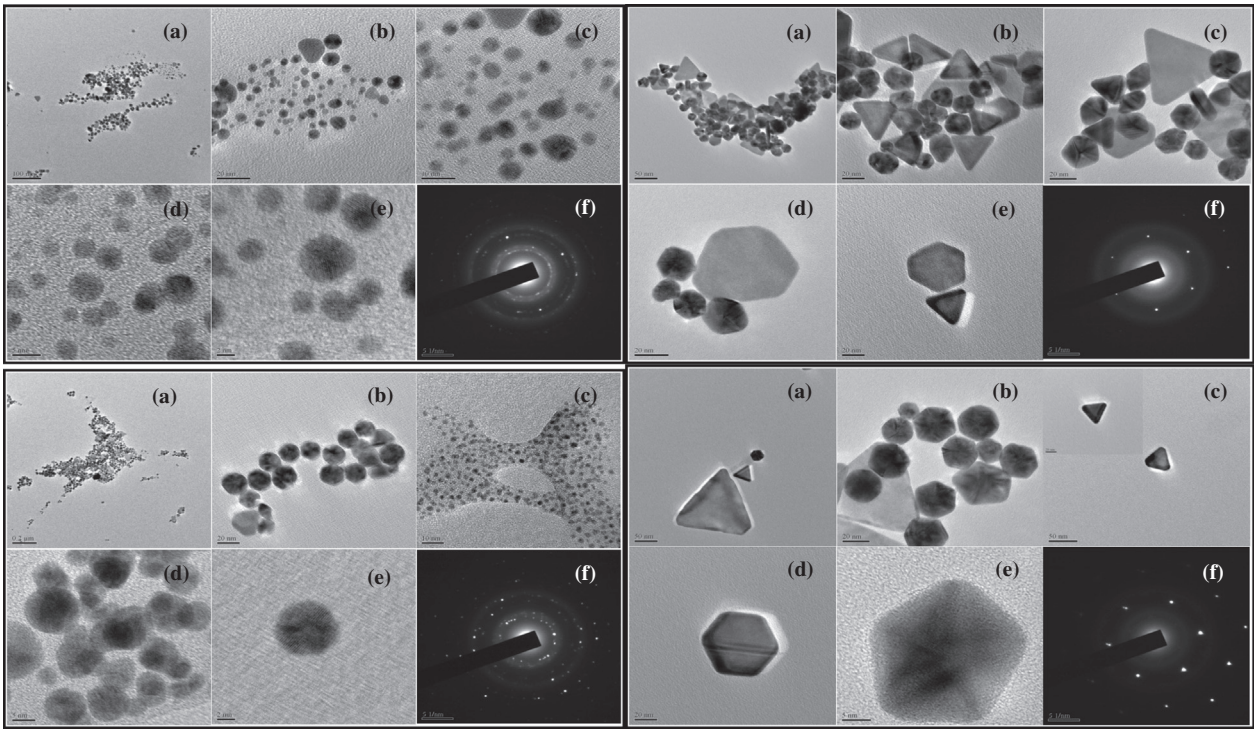

Fig. 4 A composite visual of transmission electron micrographs (a–e) showing hexagonal, pentagonal and triangular particles of gold nanoparticles formed with the extracts of the aerial parts (i and ii), and submerged parts (iii and iv) of pistia.

the electron micrographs in the spot-profile mode by focusing on the densely occupied gold nanoparticle region.

X-ray diffraction (XRD) studies

The powder XRD (X-ray diffraction) spectrum of the NPs was recorded to investigate the crystallinity of the material being analyzed. An aliquot of the pelletized GNPs was drop-casted to thin film on a glass slide and its XRD spectrum was obtained by scanning in the 2θ region, from 0° to 80°, at 0.02° per minute. Cu Kα1 radiation with a wavelength of 1.5406 Å, tube voltage 40 kV, and tube current 30 mA, was used.

Fourier transform infrared spectroscopic (FTIR) studies

FT-IR spectroscopy was done to identify the functional groups involved in the reduction, stabilization and capping of the GNPs. For this, the samples were dried and grounded with potassium bromide. The spectrum was recorded between 4000 and 400 cm^{-1} in diffuse reflectance mode, at 4 cm^{-1} resolution.

Results and discussion

Purple-red colors of different hues appeared in the otherwise colorless reaction mixture when GNP formation commenced. These colors, caused by surface plasmon resonance (SPR) in the GNPs, led to either a sharp peak in the 530–570 nm region (Fig. 1c–e) or a broader peak in the 650–800 nm region (Fig. 2a–c). In a few cases, two peaks were observed (Fig. 2d and f) – a sharp one in the 530–570 nm region and a very broad one in the near infra-red (NIR) region. Hence, in summary, basically two types of spectra were obtained, one contained a single peak and the other two peaks. In case of aerial parts, the second type of spectra occurred at metal-extract proportions of 1:6 while in case of the extracts of the submerged parts this happened at metal-extract proportions of 1:7–1:10. In all other cases, the first type of spectra was obtained. As was subsequently confirmed by electron microscopic and other studies, these two types of spectra were indicative of the formation of two types of GNPs-monodispersed spherical shaped GNPs (first type) and polydispersed mixed shaped (anisotropic) (second type).

In most cases, close to 90% of nanoparticle formation was complete by the 6th hour as thereafter the absorbance at different λ_{max} either increased only marginally or remained unchanged for several hours before beginning to decline. The decline may be due to the suspended destabilization of the nanoparticles leading to their agglomeration past the colloidal state.

In all the spectra, the presence of a single peak in the visible region is attributable to the transverse plasmon resonance (TPR) band, which arises due to the formation of spherical shaped GNPs. This was confirmed by the SEM and TEM micrographs, described below, which revealed the formation of spherical GNPs when these metal: extract combinations were used. In contrast, the presence of two peaks arose when there was anisotropic nanoparticles formation [17–19]. In this case also, SEM and TEM confirmed what the visible spectra had indicated.

Electron microscopic (SEM, Hr-SEM, TEM) and EDX studies

The SEM and Hr-SEM images of GNPs obtained from reactant mixtures, which gave single-peak (Type 1) visible spectra, exemplified by Fig. 3 showed that the particles were spherical

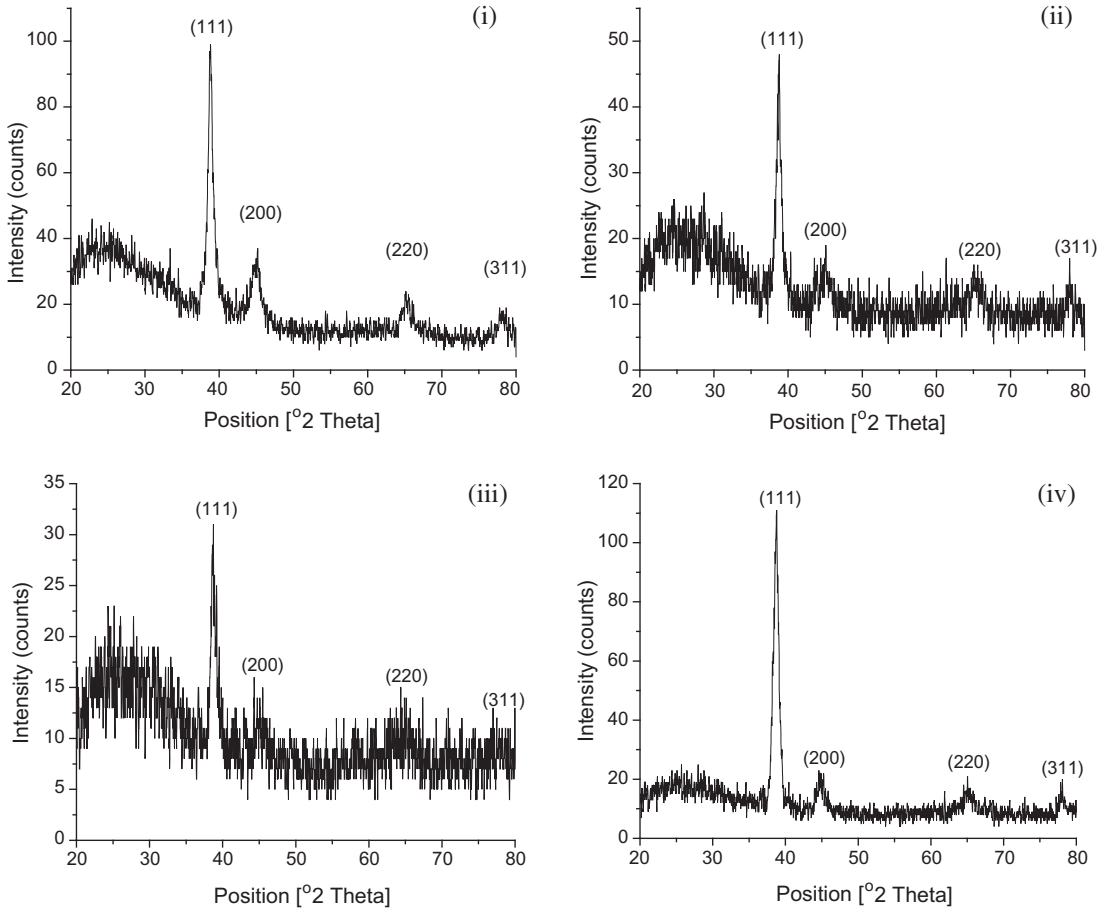

Fig. 5 X-ray diffraction spectrum of gold nanoparticles formed with the extracts of the aerial parts (i and ii), and submerged parts (iii and iv) of pistia.

in shape. The TEM images reveal that their sizes were in the range 2–40 nm (Fig. 4).

For the reactant combinations that led to GNP spectra of two peaks (Type II spectra), the SEM, Hr-SEM and TEM micrographs showed the presence of anisotropy-nanoparticles of triangular, hexagonal, pentagonal, and truncated triangular shapes (Figs. 3 and 4). The sizes of these nanoparticles ranged 20–155 nm.

A strong clear peak for gold atoms was seen in the spot-directed EDX spectrum of all the GNPs (insets of Fig. 3). The presence of carbon, nitrogen and oxygen atoms was indicated by the weaker signals. This is likely to be due to X-ray emission from proteins/enzymes present in the biomolecules that had capped the GNPs. Given that the GNPs had remained stable (retaining clear shapes) even after the pistia extract had been centrifuged out, these signals can only be from biomolecules that have remained adhered to the GNPs. An optical absorption peak at approximately 2 keV is seen, which is characteristic of gold nanoparticles [1,2].

The bright circular spots recorded in the SAED patterns (Fig. 4(i–iv) f) corresponding to the Bragg's planes confirm the crystalline nature of all types of GNPs [20].

X-ray diffraction (XRD) studies

The powder X-ray diffractograms reveal that all the GNPs had crystalline structure. The X-ray diffraction spectra (Fig. 5) showed intense peaks at 2θ position, corresponding to (1 1 1), (2 0 0), (2 2 0) and (3 1 1) Bragg's planes and denoted the fcc (face centered cubic) structure of the GNPs [21] (Table 2). The XRD patterns which match with the database of JCPDS file no. 04-0784, indicate that all types of synthesized GNPs were of pure crystalline nature. The Debye–Scherrer's equation was used to calculate the size of the GNPs on the basis of the FWHM of the (1 1 1) Bragg's reflection arising from the diffractograms [22].

The crystal sizes of the GNPs were found to be between 19.8 and 22.1 nm. In case of reactant mixtures which gave Type 1 visible spectra, the particle sizes as seen from the XRD (Fig. 5a and c) were close to the average size *ca.* 18.75 nm obtained from the electron micrographs. This were due the formation of monodispersed spherical particles. In case of reactant mixtures which gave Type II spectra, the

Table 2 2θ Position of the Bragg's plane observed from the X-ray diffractograms.

Bragg's plane	Type of GNP	(1 1 1)	(2 0 0)	(2 2 0)	(3 1 1)
2θ position	Monodispersed, spherical	38.83	45.19	65.15	77.79
		38.79	44.59	65.05	78.09
	Polydispersed, anisotropic	38.81	45.09	65.05	77.97
		38.73	44.31	64.35	76.99

particle size calculated from the XRD pattern (Fig. 5b and d) was less than that of the size determined from electron micrographs. This was probably due to the polycrystalline nature of the synthesized GNPs [23]. The ratio of optical density between the (200) and (111) Bragg's diffraction peaks was calculated to be in the range 0.04–0.16. This is lesser than the intensity ratio (i.e. 0.52) of conventional bulk gold, indicating the presence of nanoparticles with (111) facets [24].

Fourier transform infra-red spectroscopic studies

The biomolecules that could have played a role in the reduction of GNPs and the subsequent stabilization-capping of the GNPs were identified using FT-IR (Figs. 6 and 7). There is presence of strong absorption bands at 1650–1550 cm^{-1} and 1090–1020 cm^{-1} region and weaker signals in the 1550–1350 cm^{-1} region. In general, the bands found in the 1650–

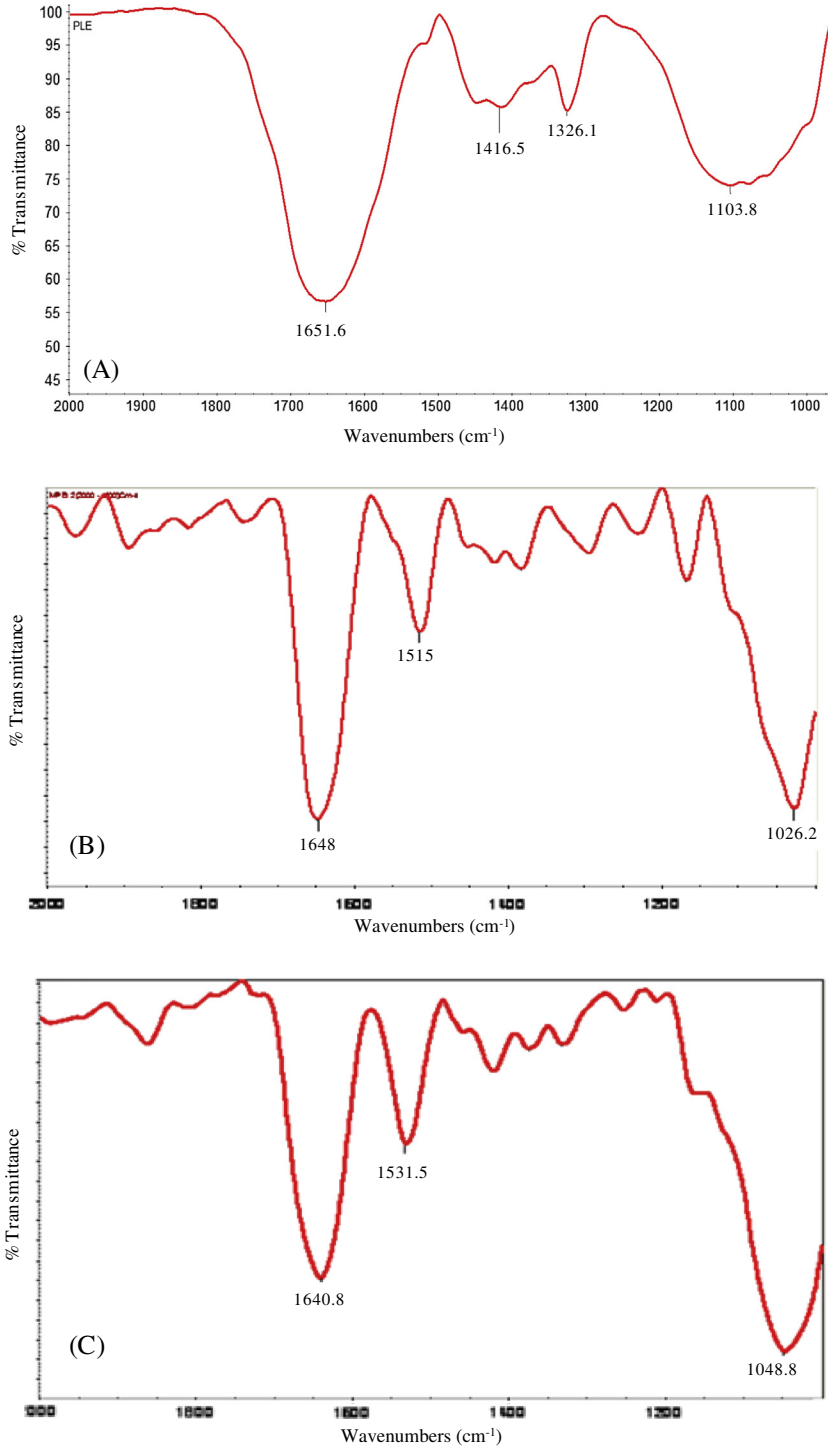

Fig. 6 FT-IR spectrum of the aerial parts (leaves) of pistia (A) and of monodispersed (B) and polydispersed (C) gold nanoparticles.

1550 cm^{-1} region correspond to secondary amine NH bend (>N—H) and the band in the 1090–1020 cm^{-1} regions is characteristic of —C—N stretching vibration due to the presence of primary amines [25,26]. The weaker signals found in 1550–1350 cm^{-1} region can be assigned to the aromatic nitro compounds. Hence, it can be inferred that primary and secondary amines found in the polypeptides of proteins could have played a role in the bioreduction and capping/stabilization of gold ions into GNPs.

Mechanism of GNP formation

From the initial studies on extracellular GNP synthesis [9,18,21] onwards, a 2-step mechanism has been proposed for GNP formation: (a) reduction of gold (iii) ions to zerovalent gold by the biomolecules present in the plant extract and, (b) the stabilization of the agglomerating gold atoms at nano-size by the enveloping of the biomolecules around them (Fig. 8). In absence of any evidence to the contrary, we believe

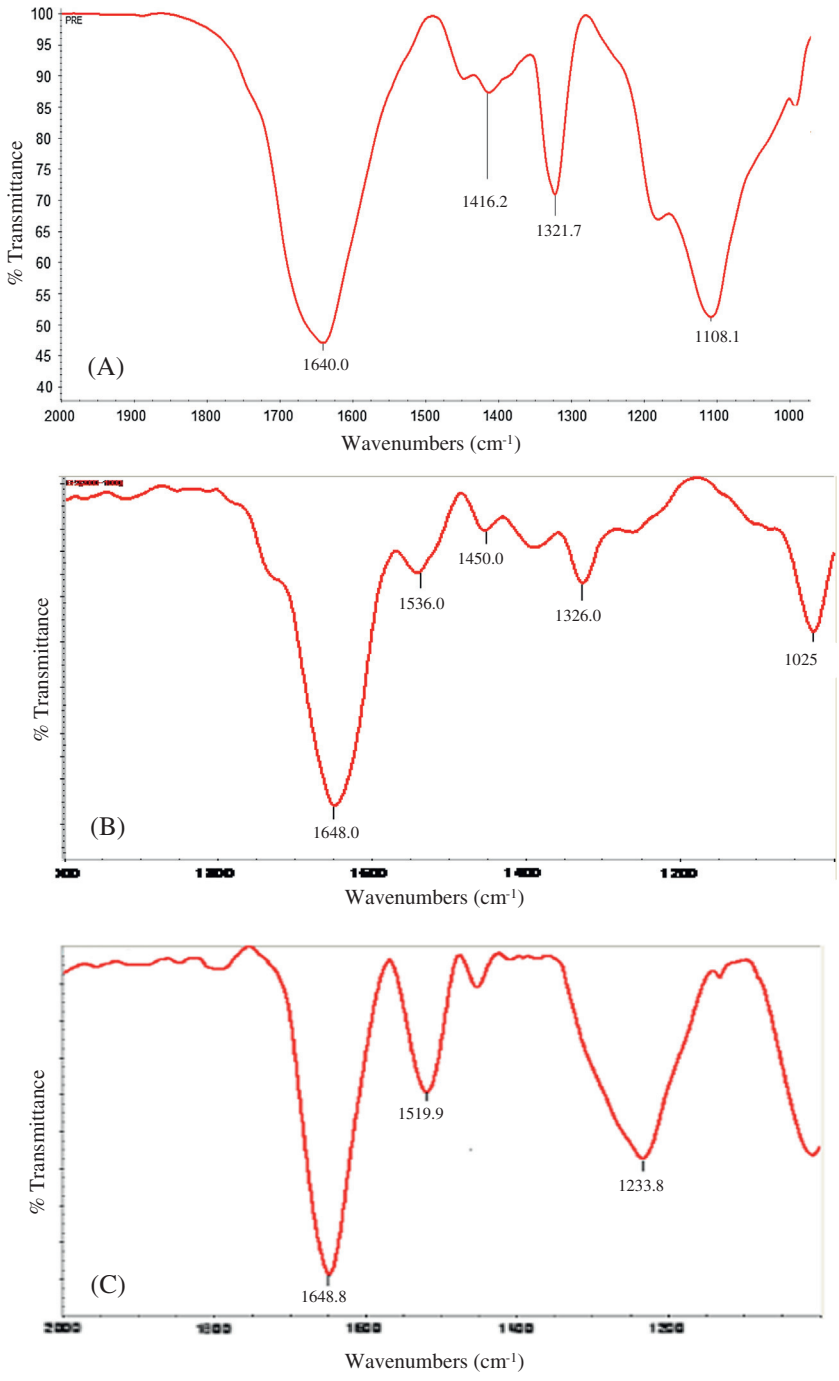

Fig. 7 FT-IR spectrum of the submerged parts (roots) of pistia (A) and of monodispersed (B) and polydispersed (C) gold nanoparticles.

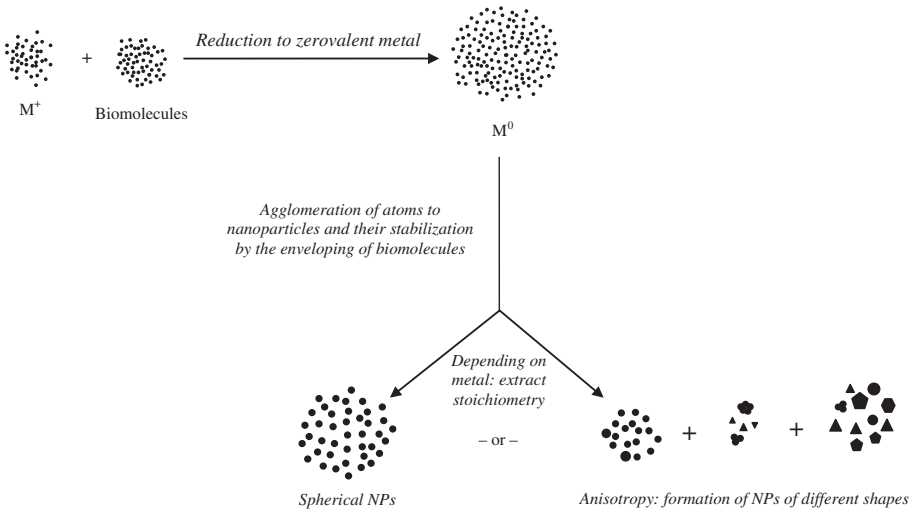

Fig. 8 Mechanism of GNP formation.

the same mechanism was operative in case of the GNPs described in this paper.

Conclusions

Aquatic weed pistia (*P. stratiotes*) was successfully utilized for the synthesis of gold nanoparticles (GNPs). Extracts from all the parts of the plant – the aerial as well as the submerged – were able to successfully induce GNP formation. SEM, TEM, FT-IR, EDX, XRD, and SAED studies reveal that based on the concentration of the extract relative to Au (III), different sizes and shapes of nanoparticles were generated. It was possible to obtain isotropic spherical or anisotropic triangular, hexagonal, pentagonal and truncated triangular shaped GNPs of different sizes. Given the fact that pistia is freely available in large quantities, with no other recognized use, the present method opens up a possibility for large-scale utilization of pistia in synthesizing GNPs in a rapid, non-polluting, energy frugal, and inexpensive manner.

Conflict of interest

The authors have declared no conflict of interest.

Compliance with Ethics Requirements

This article does not contain any studies with human or animal subjects.

Acknowledgements

The authors thank the Central Instrumentation Facility, and similar units of Pondicherry University, IIT Madras, and North-Eastern Hill University, for giving us access to various sophisticated instruments used in this study.

References

[1] Anuradha J, Abbasi T, Abbasi SA. 'Green' synthesis of gold nanoparticles with aqueous extracts of neem (*Azadirachta indica*). Res J Biotechnol 2010;5(1):75–9.
[2] Anuradha J, Abbasi T, Abbasi SA. Biomimetic synthesis of gold nanoparticles using *Aloe vera*. J Environ Sci Eng Res 2011;2:1–5.
[3] Iravani S. Green synthesis of metal nanoparticles using plants. Green Chem 2011;13:2638–50.
[4] Abbasi SA, Abbasi T, Anuradha J. A process for synthesis of metal nanoparticles from aquatic weeds. Offl J Patent Off 2012; dt: 20.04.2012: 6184.
[5] Nellore J, Pauline PC, Amarnath K. Biogenic synthesis by *Sphearanthus amaranthoids*: towards the efficient production of the biocompatible gold nanoparticles. Digest J Nanomater Biostruct 2012;7:123–33.
[6] Sujitha MV, Kannan S. Green synthesis of gold nanoparticles using Citrus fruits (*Citrus limon*, *Citrus reticulata* and *Citrus sinensis*) aqueous extract and its characterization. Spectrochim Acta Part A: Mol Biomol Spectrosc 2013;102:15–23.
[7] Mansoori GA. Synthesis of nanoparticles by fungi. United States patent application publication. Pub. No. US 2010/0055199 A1; 2010.
[8] Deshpande R, Bedre DM, Basavaraja S, Sawle B, Manjunath SY, Venkataraman A. Rapid biosynthesis of irregular shaped gold nanoparticles from macerated aqueous extracellular dried clove buds (*Syzygium aromaticum*) solution. Colloids Surf B: Biointerfaces 2010;79:235–40.
[9] Shankar SS, Rai A, Ahmad A, Sastry M. Rapid synthesis of Au, Ag, and bimetallic Au core-Ag shell nanoparticles using Neem (*Azadirachta indica*) leaf broth. J Colloid Interf Sci 2004;275:496–502.
[10] Narayanan KB, Sakthivel N. Green synthesis of biogenic metal nanoparticles by terrestrial and aquatic phototrophic and heterotrophic eukaryotes and biocompatible agents. Adv Colloid Interface Sci 2011;169:59–79.
[11] Anuradha J, Abbasi T, Abbasi SA. Facile 'phyto' fabrication of silver nanoparticles of diverse geometries with concomitant utilization of a pernicious terrestrial weed. In: Proceedings of the international conference on green technology and environmental conservation (GTEC-2011), Sathyabama University, Chennai, IEEE; 2011. p. 216–23.
[12] Abbasi SA, Abbasi T, Anuradha J, Neghi N, Pirathiba S, Ganaie SU. Gainful utilization of four otherwise worthless and problematic weeds for silver nanoparticle synthesis. Offl J Patent Off 2011; dt: 15.07.2011: 11869.
[13] Abbasi SA, Nipaney PC, Panholzer B. Biogas production from the aquatic weed pistia (*Pistia stratiotes*). Bioresour Technol 1991;37:211–4.
[14] Abbasi SA, Nipany PC. Wastewater treatment using aquatic plants. Resour Conserv 1985;12:47–55.

[15] APHA (American Public Health Association). Standard methods of water and wastewater. 22nd ed. Washington (DC), USA: American Public Health Association, American Water Works Association and Water Environment Federation Publication; 2012.
[16] Anuradha J, Abbasi T, Abbasi SA. Rapid and reproducible 'Green' synthesis of silver nanoparticles of consistent shape and size using *Azadirachta indica*. Res J Biotechnol 2011;6:69–70.
[17] Link S, El-Sayed MA. Optical properties and ultrafast dynamics of metallic nanocrystals. Annu Rev Phys Chem 2003;54:331–66.
[18] Shankar SS, Rai A, Ahmad A, Sastry M. Controlling the optical properties of lemongrass extract synthesized gold nanotriangles and potential application in infrared-absorbing optical coatings. Chem Mater 2005;17:566–72.
[19] Liz-Marzan LM. Tailoring surface plasmons through the morphology and assembly of metal nanoparticles. Langmuir 2006;22(1):32–41.
[20] Philip D. Biosynthesis of Au, Ag and Au–Ag nanoparticles using edible mushroom extract. Spectrochim Acta Part A 2009;73:374–81.
[21] Shankar SS, Ahmad A, Parsricha R, Sastry M. Bioreduction of chloroaurate ions by geranium leaves and its endophytic fungus yields gold nanoparticles of different shapes. J Mater Chem 2003;13:1822–6.
[22] Borchert H, Shevchenko EV, Robert A, Mekis I, Kornowski A, Grubel G, Weller H. Determination of nanocrystal sizes: a comparison of TEM, SAXS, and XRD studies of highly monodisperse $CoPt_3$ particles. Langmuir 2005;21:1931–6.
[23] Navaladian S, Viswanathan B, Varadarajan TK, Viswanath RP. A rapid synthesis of oriented palladium nanoparticles by UV irradiation. Nanoscale Res Lett 2008;4:181–6.
[24] Khare V, Li Z, Mantion A, Ayi AA, Sonkaria S, Voelkl A, Thunemann AF, Taubert A. Strong anion effects on gold nanoparticle formation in ionic liquids. J Mater Chem 2010;20:1332–9.
[25] Gole A, Dash C, Ramachandaran V, Mandale AB, Sainkar SR, Rao M, Sastry M. Pepsin–gold colloid conjugates: preparation, characterization, and enzymatic activity. Langmuir 2001;17:1674–9.
[26] Ogi T, Saitoh N, Nomura T, Konishi Y. Room-temperature synthesis of gold nanoparticles and nanoplates using *Shewanella algae* cell extract. J Nanoparticle Res 2009;12:2531–9.